Glycoconj J (2008) 25:863–877
DOI 10.1007/s10719-008-9149-1

Variation of acharan sulfate and monosaccharide composition and analysis of neutral *N*-glycans in African giant snail (*Achatina fulica*)

Youmie Park · Zhenqing Zhang · Tatiana N. Laremore · Boyangzi Li · Joon-Soo Sim · A-Rang Im · Mi Young Ahn · Yeong Shik Kim · Robert J. Linhardt

Received: 21 February 2008 / Revised: 8 May 2008 / Accepted: 19 May 2008 / Published online: 1 August 2008

Abstract Acharan sulfate content from African giant snail (*Achatina fulica*) was compared in eggs and snails of different ages. Acharan sulfate was not found in egg. Acharan sulfate disaccharide →4)-α-D-GlcNpAc (1→4)-α-L-IdoAp2S(1→, analyzed by SAX (strong-anion exchange)–HPLC was observed soon after hatching and increases as the snails grow. Monosaccharide compositional analysis showed that mole % of glucosamine, a major monosaccharide of acharan sulfate, increased with age while mole % of galactose decreased with age. These results suggest that galactans represent a major energy source during development, while acharan sulfate appearing immediately after hatching, is essential for the snail growth. The structures of neutral *N*-glycans released from eggs by peptide *N*-glycosidase F (PNGase F), were next elucidated using ESI-MS/MS, MALDI-MS/MS, enzyme digestion, and monosaccharide composition analysis. Three types of neutral *N*-glycan structures were observed, truncated ($Hex_{2–4}$-$HexNAc_2$), high mannose ($Hex_{5–9}$-$HexNAc_2$), and complex (Hex_3-$HexNAc_{2–10}$) types. None showed core fucosylation.

Keywords *Achatina fulica* eggs · African giant snails · Neutral *N*-glycans · Acharan sulfate · Monosaccharide composition analysis · Mass spectrometry

Abbreviations

PNGase F	peptide *N*-glycosidase F
MS	mass spectrometry
ESI	electrospray ionization
MALDI-TOF	matrix-assisted laser desorption/ ionization—time of flight
SAX	strong anion exchange
DHB	2,5-dihydroxybenzoic acid
2-PA	2-pyridylamination
GlcNAc	*N*-acetylglucosamine
GalNAc	*N*-acetylgalactosamine
CID	collision induced dissociation
Hex	hexose
HexNAc	*N*-acetylhexosamine
lacdiNAc	GalNAc β1–4 GlcNAc
IdoA	iduronic acid
GCC-SPE	graphitized carbon column—solid phase extraction
GAG	glycosaminoglycan
HPAEC-PAD	high-pressure anion-exchange chromatography with pulsed amperometric detection

Y. Park · Z. Zhang · T. N. Laremore · B. Li · R. J. Linhardt (✉)
Departments of Chemistry and Chemical Biology, Biology, and Chemical and Biological Engineering, Center for Biotechnology and Interdisciplinary Studies, Rensselaer Polytechnic Institute, Troy, NY 12180, USA
e-mail: linhar@rpi.edu

J.-S. Sim · A.-R. Im · Y. S. Kim (✉)
Natural Products Research Institute, College of Pharmacy, Seoul National University, 599 Gwanak-Ro, Gwanak-Gu, Seoul 151-742, Republic of Korea
e-mail: kims@snu.ac.kr

J.-S. Sim
National Institute of Agricultural Biotechnology, 225 Seodun-Dong, Suwon 441-707, Republic of Korea

M. Y. Ahn
Department of Agricultural Biology, National Institute of Agricultural Science and Technology, 61 Seodun-Dong, Suwon 441-100, Republic of Korea

Introduction

Glycosaminoglycans (GAGs) have a wide distribution in both vertebrates and invertebrates. GAGs, including heparin, heparan sulfate, chondroitin sulfate, dermatan sulfate, keratan sulfate, and hyaluronic acid, play many important roles in the biological systems [1–4]. GAGs, important in development, are distributed throughout the animal kingdom in the phylogenetic tree of both vertebrates and invertebrates [5]. Avian egg GAGs consist of approximately 48% hyaluronic acid and 52% galactosaminoglycan [6]. Ha *et al*. [7] have reported that the keratan sulfate content of eggshell membranes correlates with eggshell strength.

Insect GAGs have been investigated by Toyoda *et al.* [8] who report tissue-specific and stage-specific modifications of both chondroitin and heparan sulfate in *Drosophila*. Heparan sulfate has also been found in a variety of different mosquito tissues (*i.e.*, salivary glands, midguts, malpighian tubules, and ovaries) [9]. Previous research has described the presence of heparin and heparin-like compounds in the invertebrate family of mollusks [5]. Dermatan sulfate, enriched in 4, 6-*O*-disulfo galactosamine residues, has been found in embryos of the sea urchin, but the physiological implication of this oversulfated dermatan sulfate is unclear [10]. GAGs also appear during embryonic development of the mollusk *Pomacea* [11].

Acharan sulfate, a GAG that was first isolated and characterized from the body of the African giant snail, *Achatina fulica* Bowdich, has the repeating disaccharide unit, →4)-α-D-GlcN*p*Ac(1→4)-α-L-IdoA*p*2S(1→. This novel structure is related to, but significantly different from, heparin and heparan sulfate [12]. The structure of acharan sulfate is not easily explained based on the currently accepted GAG biosynthetic pathway.

Many glycans having unique structures, such as acharan sulfate, have been found in invertebrates, and may have important physiological and biological functions. The modifications of *N*-glycans in invertebrates differ from those found in vertebrates and some are immunogenic [13–15]. Neutral *N*-glycan patterns of the gastropods *Limax maximus, Cepaea hortensis, Planorbarius corneus, Arianta arbustorum* and *Achatina fulica* have been reported. The major *N*-glycans of the skin and viscera were oligomannosidic and small paucimannosidic structures, often terminated with 3-*O*-methylated mannoses [14]. The *Arion lusitanicus* egg *N*-glycans contain mainly oligomannosidic structures as well as some paucimannosidic structures modified by xylose or α(1-6)-fucose, but no methylation was detected [13]. Dreon *et al.* [16] characterized the major egg glycolipoproteins from the perivitellin fluid of the apple snail, *Pomacea canaliculata*. Hybrid and high mannose type *N*-glycan structures were suggested by lectin affinity studies. The characteristic features of egg core *N*-glycans from *Schistosoma* are the (β1–2)-xylose at the central β-mannosyl residue and/or (α1–3/α1–6) fucose at chitobiose core [17]. The hemocyanin *N*-glycan structures from marine snail *Rapana venosa* have high-mannose and complex glycans with unknown and unusual acidic terminus [18]. A core α(1–3) fucosyltransferase, from the snail *Lymnaea stagnails,* was characterized that is involved in the synthesis of complex-type *N*-glycans [19].

Snails also have branched galactan polysaccharides, composed of D- and L-galactosyl residues, which are synthesized in the albumin glands and eggs of *Achatina fulica* [20, 21]. These polysaccharides apparently provide nutrition for the growing embryos or the freshly hatched snails. Snail galactans from *Biomphalaria*, from albumin glands and freshly collected eggs, are mainly composed of D-galactopyranose. *Biomphalaria* galactans contain more β(1–3) linkages than β(1–6) linkages [22].

In this study we seek to better understand the biosynthetic pathway of acharan sulfate and the role it plays in *Achatina fulica* development, before and after hatching. We also study changes in monosaccharide composition and *N*-glycan structure in eggs and snails.

Materials and methods

Materials

The giant African snails *Achatina fulica* and their eggs were obtained from a greenhouse at Yong-In, Kyung-Gi-Do, Republic of Korea. Heparin lyase II (acharan sulfate lyase) was purified from *Bacteroides stercoris* HJ-15 [23, 24]. Fucose (Fuc), rhamnose (Rha), galactosamine (GalN), glucosamine (GlcN), galactose (Gal), glucose (Glc), mannose (Man), xylose (Xyl), fructose (Fru), arabinose (Ara), 2-aminopyridine, sodium cyanoborohydride, 2,5-dihydroxybenzoic acid (DHB), chitinase from *Streptomyces griseus*, α-mannosidase from Jack bean, trifluoracetic acid (TFA), mercaptoethanol, trichloroacetic acid, cetylpyridinium chloride, and Triton X-100 were purchased from Sigma-Aldrich (St. Louis, MO, USA). β-*N*-Acetylhexosaminidase cloned from *Streptomyces plicatus* and PNGase F were from New England BioLabs (Ipswich, MA, USA). Graphitized non-porous carbon (Supelclean™ ENVI-Carb SPE column: 1 ml volume, 100 mg bed weight, and bulk resin) was from Supelco (Bellefonte, PA, USA). Alcalase and Bio-Gel P2 resin were from Novozymes (Krogshoejvej, Bagsvaerd, Denmark) and Bio-Rad (Hercules, CA, USA), respectively. All other reagents used were analytical grade.

Purification of acharan sulfate from snail eggs and snails

Acharan sulfate was purified from *Achatina fulica* eggs and snails of different ages according to the methods described previously with minor modification [12]. Briefly, snail eggs and snails were cleaned, lyophilized, and ground. The dried powder was suspended in 50 mM sodium carbonate buffer (pH 7.0) containing 1% (*v*/*v*) alcalase (2.4 Anson units/g, Novo) and shaken at 60°C for 24 h at 150 rpm in the shaking incubator. After boiling for 10 min, cooling at 4°C, and filtering, trichloroacetic acid solution (6.1 MN) was mixed with the filtrate to be a final concentration of 5% (*v*/*v*). Proteins were denatured at 4°C for 30 min and removed by centrifugation at 6,296 *g* for 30 min at 4°C. Then, three volumes of cold ethanol were added to the supernatant and the suspension was stored at 4°C overnight. The precipitate obtained after centrifugation at 6,296 *g* for 30 min at 4°C was dried, dissolved with water, mixed with cetylpyridinium chloride (final concentration 1%, *w*/*v*), and stored at room temperature for 1 h. After centrifugation at 6,296 *g* for 30 min at 4°C, the pellet was dissolved with 2.5 M NaCl at 45°C for 30 min at 200 rpm in the shaking incubator and mixed with four volumes of cold ethanol. The pellet was collected after centrifugation at 6,296 *g* for 30 min at 4°C, dissolved with water, dialyzed (MWCO 3.5 kDa, Spectrum® laboratories), and freeze-dried.

Enzymatic depolymerization of acharan sulfate with heparin lyase II

Standard acharan sulfate from snail body was dissolved in water to make a stock solution (10 mg/ml). Fifteen microliters of sample and standard AS solution were individually mixed with 255 μl of 50 mM sodium phosphate buffer (pH 7.0) containing 100 mM NaCl. The samples were depolymerized with 30 μl of heparin lyase II (56 mIU/μl) overnight at 35°C. After heating for 5 min and filtering through 0.45 μm filters, the depolymerization mixtures (100 μl) were subjected to HPLC. Acharan sulfate disaccharides generated by enzymatic depolymerization were analyzed on a 0.46×25 cm, 5 μm particle size strong-anion exchange (SAX) analytical column from Thermo Hypersil-Keystone (Bellefonte, PA, USA) using the ÄKTA Purifier controlled by UNICORN software 5.01 from Amersham Pharmacia (Uppsala, Sweden). After sample injection, the column was washed with water (pH 3.5) for 4.155 min corresponding to 1 CV. Then, the linear gradient of 0–1.0 M NaCl (pH 3.5) for 41.55 min (10 CV) was performed at a flow rate of 1.0 ml/min with detection at 232 nm. The content (%) of acharan sulfate in samples was calculated as total peak area of the disaccharides by comparing with that of standard acharan sulfate.

Liberation of snail egg *N*-glycans by PNGase F

Snail egg water extract (1 g) was dissolved in 20 ml of 100 mM sodium phosphate buffer (pH 7.6) containing 5 mM mercaptoethanol and 0.1% (*v*/*v*) Triton X-100. After boiling for 10 min and cooling at room temperature, the solution was mixed with PNGase F (4 μl, 500 U/μl) and incubated at 37°C for 24 h. The supernatant was obtained by centrifugation at 3,720 *g* for 30 min at 4°C and then freeze-dried. For desalting, lyophilized powder was dissolved in water and then loaded on a column (100×2.5 cm) packed with 380 ml of Bio-Gel P2 resin sufficiently equilibrated with water. After loading the sample, the elution profile of fractions was monitored at 210 nm and main fractions were pooled and freeze-dried. To purify *N*-glycans, 10 g of Supelclean™ ENVI-Carb SPE bulk packing resin was washed with water and packed into a column (20×1.5 cm, BIO-RAD) as previously described [25, 26]. The column was then conditioned with 150 ml (five column volumes) of 80% (*v*/*v*) acetonitrile containing 0.1% (*v*/*v*) TFA, followed by 450 ml of water. After loading the sample solution, the column was washed with 120 ml of water and the flow rate was maintained at 0.5 ml/min. Neutral *N*-glycan fractions eluted with 90 ml of 20% (*v*/*v*) acetonitrile were collected, evaporated at 50°C, and freeze-dried. Acidic *N*-glycan fractions were eluted with 90 ml of 40% (*v*/*v*) acetonitrile containing 0.05% (*v*/*v*) TFA and treated under the same conditions as the neutral *N*-glycan fractions. Neutral *N*-glycans treated with β-*N*-acetylhexosaminidase, chitinase, and α-mannosidase treated and 2-aminopyridylated neutral *N*-glycans were purified by GCC-SPE (100 mg bed weight, 1 ml) as described above.

β-*N*-Acetylhexosaminidase, chitinase, and α-mannosidase digestion of neutral *N*-glycans

For β-*N*-acetylhexosaminidase digestion, neutral *N*-glycan 100 μg was freeze-dried and re-dissolved in 450 μl water. The reaction buffer (10×, 500 mM sodium citrate, pH 4.5), 50 μl was added to the *N*-glycan solution. β-*N*-acetylhexosaminidase (5,000 U/ml, 10 μl or 20 μl) was added to *N*-glycan solution and incubated at 37°C water bath for 1 h. For chitinase digestion, neutral *N*-glycan 100 μg was freeze-dried and re-dissolved in 200 μl of 50 mM sodium citrate, pH 5.0. Chitinase (200 mU/ 20 μl) was added and incubated at 37°C water bath overnight. For α-mannosidase digestion, neutral *N*-glycan (1.4 mg) was dissolved in 500 μl water. α-Mannosidase enzyme suspension (3.0 M $(NH_4)_2SO_4$ and 0.1 mM zinc acetate pH 7.5) 1 μl was added and incubated at 37°C water bath for 1 hr. After incubation, enzymes were inactivated by boiling for 3 min. Then enzyme-treated *N*-glycans were purified by GCC-SPE prior to MALDI MS analysis.

Pyridylamination of neutral *N*-linked glycans

The neutral *N*-glycans (0.1–1 mg) were dried and dissolved in 40 μl water. A mixture of methanol (350 μl) and glacial acetic acid (80 μl) was combined with 2-aminopyridine (184 mg) and sodium cyanoborohydride (35 mg) and this solution was mixed in vortex mixer and used immediately. The *N*-glycan oligosaccharide solution, 40 μl was added to the above 2-aminopyridine solution, 40 μl, and the mixture was heated for 15 h at 80°C in a dry heating block. The reaction was stopped by adding 500 μl of water, cooled to room temperature and applied to a GCC-SPE cartridge. The original water extract of eggs prior to PNGase F digestion was pyridylaminated using the same procedure.

Preparative-HPLC of pyridylaminated *N*-glycans

Shimadzu HPLC system (SLC-10A system controller, LC-10Ai pump, and SPD-10Ai UV–Vis detector) was used for the separation of 2-PA labeled neutral *N*-glycans. Reverse-phase HPLC was performed on a C18 column from Supelco (250×21.2 mm, 5 μm) with a gradient elution (A: 100 mM ammonium acetate, pH 4.0; B: 100 mM ammonium acetate, pH 4.0, containing 0.5% 1-butanol) [27]. The column was equilibrated with 5% B. The gradient system was as follows: 0–5 min 5% B, 5–35 min 5–18% B, 35–75 min 18–50% B, 75–85 min 50–100% B, and 85–90 min 100% B. The flow rate was 4 ml/min with UV detection at 315 nm.

Mass spectrometry

MALDI-TOF mass spectrometry was performed on a Voyage-DE™ STR Biospectrometry Workstation (Applied Biosystems Inc, Germany) equipped with a nitrogen laser and on a Bruker Ultraflex-III TOF-TOF mass spectrometer (Bruker, Billerica, MA, USA) equipped with Nd:YAG laser. Mass spectra were acquired in the positive reflector mode using DHB as a matrix. MALDI-MS/MS mass spectra were acquired in LIFT mode on a Bruker Ultraflex III TOF–TOF instrument with the ion sources 1 and 2 set to 8 kV and 7.2 kV respectively and the lens voltage of 3.6 kV. LIFT 1 and 2 voltages were 19 kV and 2.6 kV, respectively, reflector 1 was at 29.5 kV and reflector 2 was at 13.8 kV. Precursor ion was selected within ±5 Da window. A sufficient post-source fragmentation of the precursor ion under standard vacuum conditions made the use of collision gas unnecessary. LIFT mass spectra were calibrated using bradykinin (1–7) and angiotensin I and II as standards.

LC-ESI-MS analyses were performed on Agilent 1100 LC/MSD instrument (Agilent Technologies, Wilmington, DE) equipped with an ion trap, binary pump, and a UV detector. The column was a 5 μm Agilent Zorbax SB-C18 (0.5×250 mm) from Agilent Technologies. Eluent A was 100 mM ammonium acetate pH 4.0, and eluent B was 100 mM ammonium acetate pH 4.0 containing 0.5% 1-butanol. *N*-glycans and 2-PA labeled *N*-glycans were injected by auto-sampler. The gradient was as follows: 0–60 min 5–100% B; 60–70 min 100% B; 70–90 min 5% B, at the flow rate of 10 μl/min. Mass spectra were obtained using an Agilent 1100 series LC/MSD trap (Agilent Technologies, Wilmington, DE, USA). The electrospray was set in alternating negative and positive ionization modes with the skimmer potential −40.0 and 40.0 V, capillary exit −120.5 and 120.5 V, respectively, and a source temperature of 325°C to obtain maximum abundance of the ions in a full scan spectra (150–1,500 Da, 10 full scans/s). Nitrogen was used as a drying (5 l/min) and nebulizing gas (20 p.s.i.). Auto MS/MS was also performed in alternating mode using an estimated cycle time of 0.07 min. Total ion chromatograms (TIC) and mass spectra were processed using Data Analysis 2.0 (Bruker software).

Monosaccharide composition analysis by HPAEC-PAD

N-glycans (100 μl, 10 mg/ml) from snail eggs and acharan sulfate (100 μl, 10 mg/ml) from snails were lyophilized and hydrolyzed by treatment with 400 μl of 2 M TFA at 100°C for 4 h. After cooling at room temperature, TFA was removed by centrifugal evaporation system (Genevac EZ-2 plus, Genevac, UK) at room temperature. Hydrolyzed samples were dissolved in water (200 μl), filtered through a 0.2 μm microspin column (Nanosep MF Centrifugal Devices, Pall Corporation, Michigan), and injected into the HPAEC-PAD system. Monosaccharide peaks from *N*-glycans and acharan sulfate were confirmed by the injection of a mixture of authentic monosaccharide samples (250, 500, 1,000, 2,000, 3,000, and 4,000 pmol) including Fuc, Rha, GalN, GlcN, Gal, Glc, Man, Xyl, and Fru, and individually quantified based on the calibration curves. HPAEC-PAD analyses were performed on the Bio-LC system (Dionex, Sunnyvale, CA, USA) equipped with gradient pumps (GS50, Dionex), an autosampler, and a pulsed amperometric detector (ED50A, Dionex) with a gold working electrode. PeakNet 6.3 software (Dionex) was used to control the instrument and collect data. Separation of monosaccharides was performed on a CarboPac™ PA−1 column (4×250 mm, Dionex) at 1.0 ml/min. 18 mM NaOH (eluent A) and 1 M NaOH containing 1 M sodium acetate (eluent B) were used as follows: 0–25 min: 0% B; 25–40 min: 30% B; 40–70 min: 0% B. The pulse potential of detector was set at $E1=0.05$ V ($t_1=120$ ms), $E2=0.60$ V ($t_2=120$ ms), $E3=-0.80$ V ($t_3=300$ ms) with an output range of 1–3 knA. The mobile phases used for HPAEC-PAD were filtered through a 0.45 μm membrane filter prior to analyses (Millipore, Bedford, MA, USA).

Results

Acharan sulfate from snail eggs and snail

Snail eggs and snails of differing age (Fig. 1) were collected and acidic polysaccharide was recovered from these samples. Polysaccharide corresponding to acharan sulfate was determined (Table 1). The yield of acidic polysaccharides from snails increased with increasing age. The acharan sulfate content (%) in the recovered acidic polysaccharides was determined by treatment with heparin lyase II followed by disaccharide analysis. Acharan sulfate content (%), quantitatively analyzed by heparinase II digestion followed by SAX-HPLC, also increased with increasing age (Table 1). However, snail egg acidic polysaccharides did not contain acharan sulfate indicating the presence of other acidic polysaccharides in snail eggs. When acidic polysaccharides from eggs were treated with heparin lyase I, II, III, and chondroitinase ABC, no disaccharide or oligosaccharide products were detected. Thus, it is unlikely that these acidic polysaccharides are GAGs. These acidic polysaccharides instead might come from negatively-charged mucins giving snail eggs their very high viscosity.

Monosaccharide composition analysis

The monosaccharide composition analysis of the neutral and acidic *N*-glycans in snail eggs was next determined (Table 2). GalN (20.71 mol %), GlcN (14.41 mol %), Gal (48.32 mol %), Glc (4.84 mol %), and Man (11.72 mol%) were detected in neutral *N*-glycans. In acidic *N*-glycans, GalN (22.36 mol%), GlcN (9.31 mol%), Gal (64.08 mol%), and Man (4.25 mol%) were detected. Gal mole % was the highest in both neutral and acidic *N*-glycans from eggs. Seven monosaccharides were observed in snails; Fuc, Rha, GlcN, GalN, Gal, Glc, and Man. The mole % of each monosaccharide is summarized in Table 2.

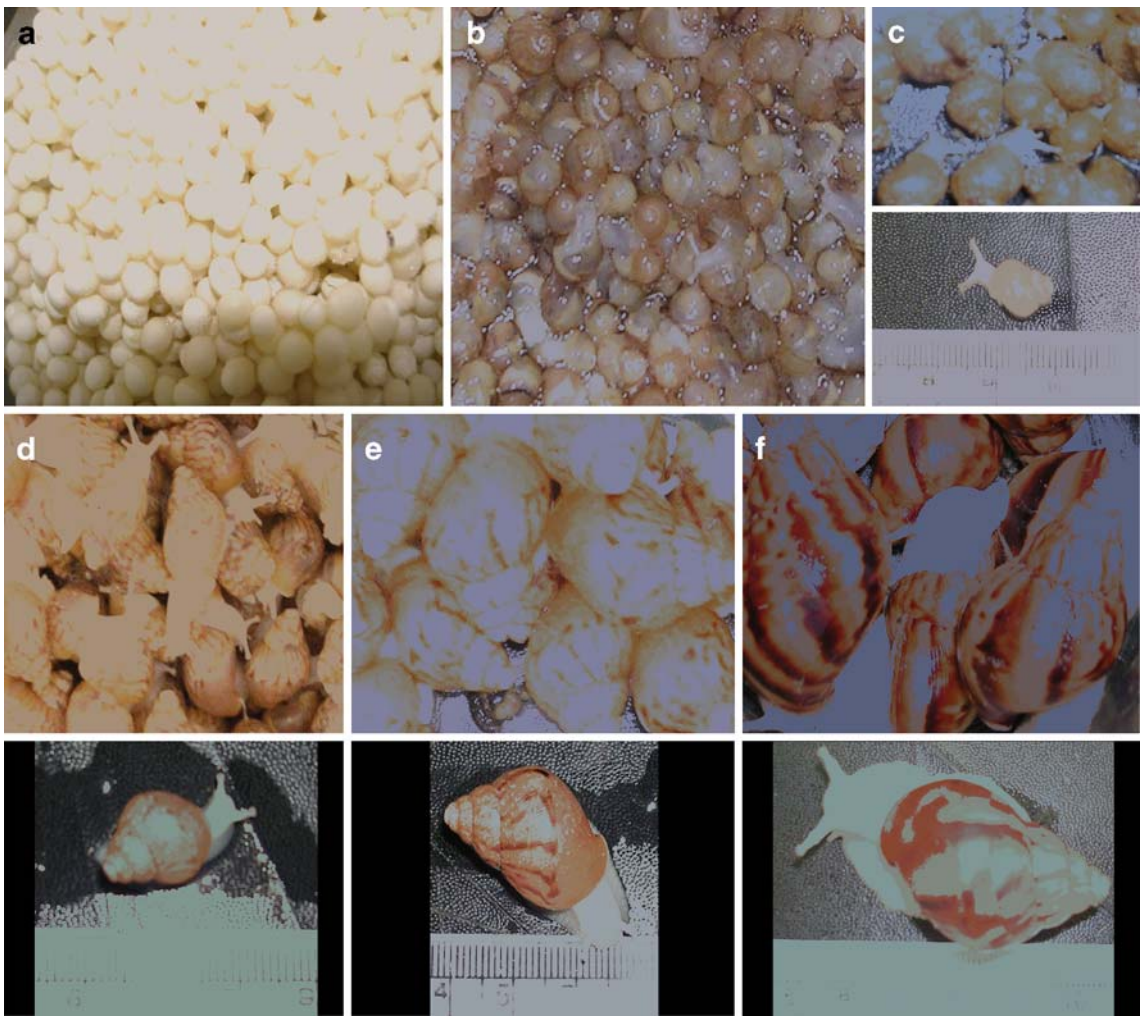

Fig 1 Pictures of **a** snail eggs, **b** snails (3 days), **c** snails (7–10 days), **d** snails (15–20 days), **e** snails (45–60 days), and **f** snails (~120 days; unit: centimeters)

Table 1 AS contents (%) in snail eggs and snails

Source	Yield (%) of acidic polysaccharides (%)	Acharan sulfate content (%) in acidic polysaccharides
Snail eggs	0.03	ND
Snails (3 days)	0.13	21.3
Snails (7–10 days)	0.59	45.0
Snails (15–20 days)	0.79	46.5
Snails (45–60 days)	0.78	65.3
Snails (~120 days)	0.87	73.7

The mol % of Gal decreased as snails grew (Table 2). But GlcN appeared at day 3 and continuously increased. At day 15–20, the mole % of Gal and GlcN was nearly the same, and at day 120, GlcN was the major monosaccharide in snails. It appears that most GlcN comes from GlcNAc, which is a major component of acharan sulfate disaccharide, →4)-α-D-GlcN*p*Ac(1→4)-α-L-IdoA*p*2S(1→ [12]. These results correlate well with the increasing content of acharan sulfate (Table 1). The mole % of Fuc varied from 13.01–17.31%, suggesting fucosylation of snail *N*-glycans and *O*-glycans. Rha began appearing at day 3 and was highest at day 15–20 (7.18 mol%). Glc increased with age from 4.00% to 17.9%, and Man varied but was the lowest among the monosaccharides determined.

Analysis of the neutral *N*-glycans in the eggs by MALDI-TOF-MS and LC-ESI-MS

MALDI-MS spectrum of the underivatized neutral *N*-glycans ($[M + Na]^+$) and ESI-MS spectrum of 2-PA derivatized neutral *N*-glycans ($[M + H]^+$) are presented in Fig. 2a and b, respectively. The trimannosyl chitobiose core (Hex_3-$HexNAc_2$) corresponds to an ion at *m/z* 933.4 in MALDI-MS. However, no fucosylated *N*-glycans were released by treatment with PNGase F. In addition, monosaccharide compositional analysis confirmed that there was no detectable fucose in *Achatina fulica* egg *N*-glycans (Table 2). No terminal methylation was observed on the trimannosylchitobiose core in the *N*-glycans obtained from eggs, however, methylation on trimannosylchitobiose core as well as xylosylation from *Achatina fulica* tissues had been previously reported [14].

The nonfucosylated trimannosylchitobiose core carries two major types of antennae based on the observed *m/z* values from MALDI-MS. One carries Hex residues ($Hex_{2–9}$-$HexNAc_2$), and the other carries HexNAc residues (Hex_3-$HexNAc_{2–10}$; Fig. 2a). Next, the 2-PA labeled neutral *N*-glycans were analyzed by ESI-MS (Fig. 2b). The protonated ions of *N*-glycans as well as hexose repeats (Hex_2-PA, Hex_3-PA, Hex_4-PA, and Hex_5-PA) are observed.

Characterization of truncated and high mannose type *N*-glycans

The peaks observed in MALDI-MS (Fig. 2a) suggest a range of high-mannose structures that have repeating mannose residues in their antennae ($Hex_{5–9}$-$HexNAc_2$). The digestion with α-mannosidase resulted in the diminution of the peaks in MALDI-MS confirming that they corresponded to high mannose structures.

Truncated structures corresponding to Hex_{2-4}–$HexNAc_2$ are also observed (Fig. 2a and b). ESI-MS/MS of protonated, unlabeled *N*-glycans has been reported [28], suggesting it would be worthwhile to perform MS/MS of protonated, 2-PA labeled *N*-glycans. The fragmentation mass spectra are annotated using the nomenclature of Domon and Costello [29]. The positive mode of ESI-MS/MS of Hex_3-$HexNAc_2$-PA is shown in Fig. 3a, in which major fragments resulting from Y- and Z-cleavages as well as a B-cleavage were observed. A fragment, corresponding

Table 2 Mol (%) of neutral and amino monosaccharides from snail eggs and snails

	Snail eggs		Snails with different age (days)					
Sugars	Neutral *N*-glycans	Acidic *N*-glycans	0 (eggs)	3	7–10	15–20	45–60	~120
Fuc	ND	ND	ND	13.0	17.3	15.5	16.6	13.9
Rha	ND	ND	ND	2.85	6.91	7.18	5.58	4.45
GalN	20.7	22.4	3.49	9.02	7.28	7.86	7.55	7.41
GlcN	14.4	9.31	ND	13.7	27.6	26.5	35.0	37.0
Gal	48.3	64.1	96.5	57.4	29.8	27.8	24.8	19.3
Glc	4.84	ND	ND	4.00	8.83	12.6	10.6	17.9
Man	11.7	4.25	ND	ND	2.32	2.63	ND	ND

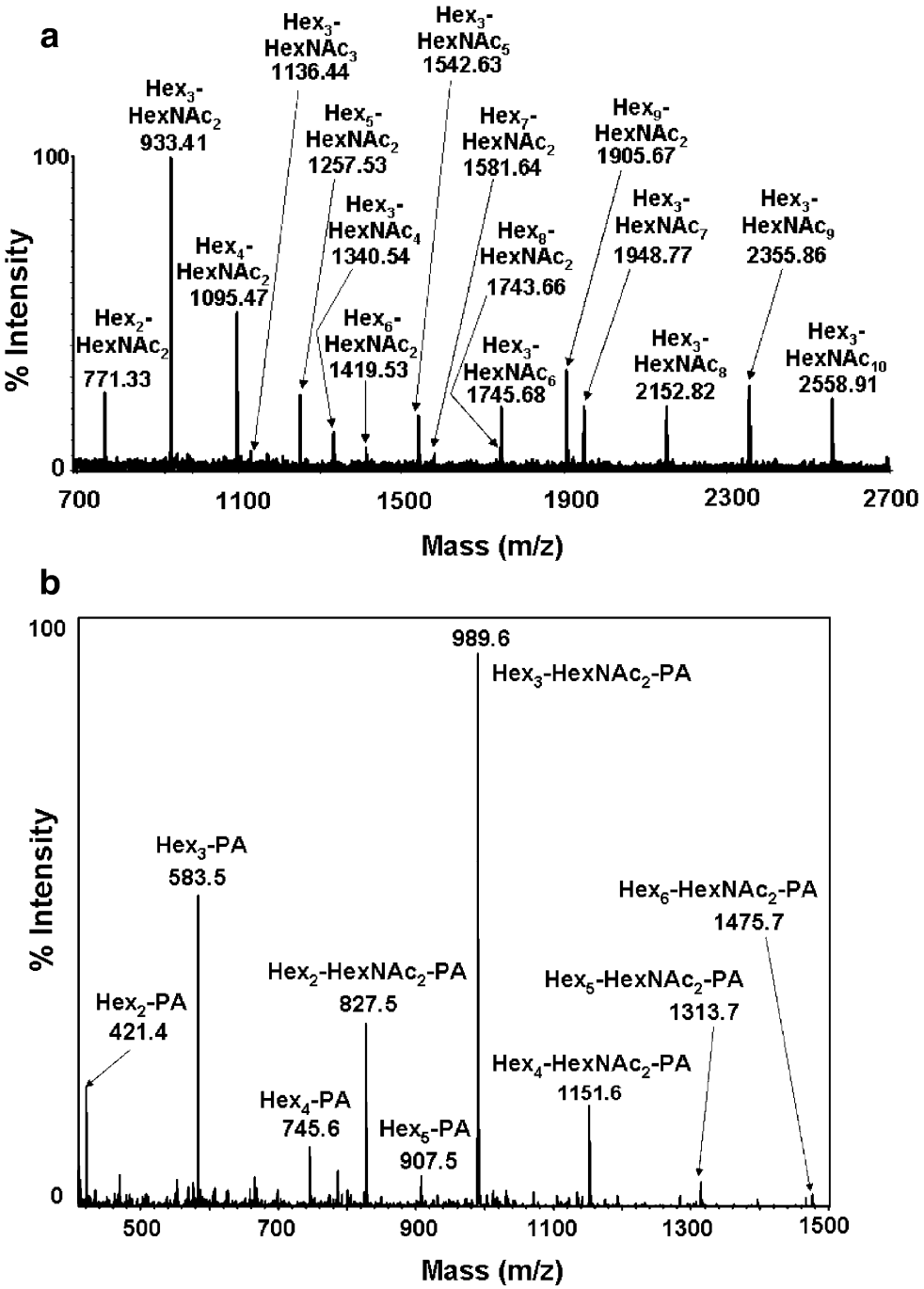

Fig. 2 Neutral *N*-glycans released by PNGase F **a** MALDI-MS of sodiated ions, and **b** ESI-MS of 2-PA labeled neutral *N*-glycans of protonated ions

to the reducing-terminal GlcNAc residue with 2-PA (Y_1) was observed with relatively high intensity. However, breakage of the bond between 2-PA and GlcNAc at the reducing end is less likely as this fragmentation requires higher energy. The major ion in this mass spectrum is from the loss of a mannose residue from the non-reducing terminus (Y_3). In the negative ion mode, Hex_3-$HexNAc_2$-PA was fragmented to produce more complicated patterns containing glycosidic bond cleavage products (Y-, B- and C-) containing sequence information and cross-ring cleavage ions (X-, and A-; data not shown). The structure of Hex_4-$HexNAc_2$-PA was also confirmed by the same method and its ESI-MS/MS is shown in Fig. 3b. The proposed structures of both high mannose and truncated type *N*-glycans are summarized in Table 5. The observed *m/z* values are well correlated with the theoretical values.

Characterization of complex type *N*-glycans

The other series of neutral *N*-glycans was composed of HexNAc repeats with 1–8 HexNAc residues at trimannosyl chitobiose core (Fig. 2a). Incubation with chitinase showed

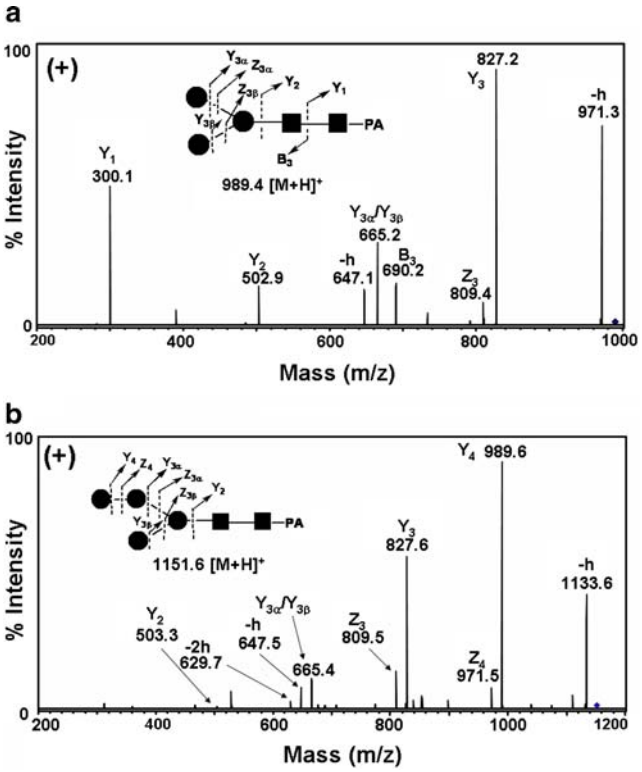

Fig. 3 ESI-MS/MS of 2-PA labeled *N*-glycans in positive ion mode. **a** Trimannosyl-chitobiose core (Hex_3-$HexNAc_2$-PA), and **b** truncated *N*-glycans (Hex_4-$HexNAc_2$-PA). *Square* GlcNAc, *circle* Man

that the HexNAc repeat in the antennae was resistant to enzymatic digestion, excluding the possibility that this repeat was GlcNAc β1→4 GlcNAc. However, incubation with β-*N*-acetylhexosaminidase removed HexNAc residues in the antennae indicating the presence of lacdiNAc in the complex type structures (Table 3, and Scheme 1) [30]. Monosaccharide composition analysis of neutral *N*-glycans shows the presence of *N*-acetylgalactosamine (see Table 2). This result supports the presence of the lacdiNAc-type biosynthetic pathway in the snail egg neutral *N*-glycans. Furthermore, the peaks corresponding to the HexNAc repeats (Hex_3-$HexNAc_{10}$, Hex_3-$HexNAc_9$, Hex_3-$HexNAc_8$, and Hex_3-$HexNAc_7$) disappeared after treatment with β-*N*-acetylhexosaminidase, and the relative intensities of the peaks (Hex_3-$HexNAc_6$, Hex_3-$HexNAc_5$, and Hex_3-$HexNAc_3$) were reduced. By increasing the amount of enzyme 2-fold, the relative intensities of these peaks were further reduced (Table 3). Thus, it is reasonable to conclude that the HexNAc residues of *N*-glycan antennae are β-linked.

Two unlabeled (Hex_3-$HexNAc_4$ and Hex_3-$HexNAc_6$) and four of 2-PA labeled (Hex_3-$HexNAc_3$-PA, Hex_3-$HexNAc_4$-PA, Hex_3-$HexNAc_5$-PA, and Hex_3-$HexNAc_6$-PA) complex-type *N*-glycans were analyzed by MALDI-TOF–TOF. A representative tandem mass spectrum of 2-PA labeled *N*-glycan (Hex_3-$HexNAc_5$-PA), $[M + Na]^+$ is shown in Fig. 4. A general feature of fragmentation of labeled glycans in MALDI is that B- and Y-cleavage ions are extensively observed from $[M + Na]^+$ ions. The loss of the reducing end GlcNAc residue from the parent molecular ion was observed in the unlabeled compounds (B-cleavage; data not shown). The 2-PA labeled GlcNAc loss from the parent molecular ion was also observed in labeled compounds (B-cleavage). The observed signal at *m/z* 225.8 was the sodiated ion of HexNAc. The assignments of molecular ions and characteristic fragment ions observed in MALDI-MS/MS are presented in Table 4. The abundant signals correspond to *N*-glycans that have compositions consistent with trimannosyl-chitobiose cores to which HexNAc residues are attached. The ion at *m/z* 354.7 corresponds to ^{3,5}X-cross ring cleavage of $HexNAc_2$ $+Na^+$, which most likely is a fragment of GalNAc-GlcNAc moiety from the antennae. Okamoto *et al.* [31] reported fragmentation pattern of 2-PA labeled maltopentose in PSD-MALDI using DHB matrix., in which they observed the products of B-, Y-, and ^{3,5}X-cross ring cleavages from sodiated parent ions; our results are consistent with this report. Table 5 provides a summary of proposed complex-type (lacdiNAc) *N*-glycans. The observed *m/z* values are correlated well with the theoretical values. Due to the presence of galactan and glucan contaminants in neutral *N*-glycan preparations, it was not possible to isolate pure *N*-glycans for analysis. Thus, there is more than one possible structure for each *m/z* based on the currently accepted *N*-glycan biosynthetic pathway.

Characterization of the hexose repeats in the *N*-glycan preparation

In addition to neutral *N*-glycans, oligosaccharides containing hexose repeats were observed. The original water extract, which was used for PNGase F digestion, was subjected to 2-PA labeling. LC-ESI-MS data showed the presence of hexose repeats in the original water extract (data not shown), which co-purified with neutral *N*-glycans. These oligosaccharides (Hex_2, Hex_3, Hex_4, and Hex_5) were observed in both MALDI-MS and ESI-MS.

Table 3 Comparing relative peak intensities on β-*N*-acetylhexosaminidase digestion of complex type *N*-glycans

glycan composition	no enzyme	Enzyme	Enzyme (×2)
Hex_3-$HexNAc_{10}$	0.57	–	–
Hex_3-$HexNAc_9$	0.48	–	–
Hex_3-$HexNAc_8$	0.35	–	–
Hex_3-$HexNAc_7$	0.30	–	–
Hex_3-$HexNAc_6$	0.23	0.1	0.03
Hex_3-$HexNAc_5$	0.23	0.1	0.02
Hex_3-$HexNAc_4$	0.16	0.43	0.37
Hex_3-$HexNAc_3$	0.10	0.06	0.03
Hex_3-$HexNAc_2$	1.0	1.0	1.0

Hex_3-PA was purified by a preparative RP-HPLC (retention time 40.5 min). The positive-ion mode ESI-MS/MS of Hex_3-PA showed fragments from Y-cleavages (Y_2 and Y_1) and a Z_1-cleavage as major ions (Fig. 5a). In the negative mode, Z-type cleavages (Z_2 and Z_1-h) and a C_2-cleavage were observed as well as a $^{0,2}A_2$ cross-ring cleavage (Fig. 5b). The presence of an ion at *m/z* 340.9 suggests that the structure is linear, because this ion could not be generated by C_2 cleavage in a branched structure. The proposed structures are summarized in Table 5. The observed *m/z* values are correlated well with the theoretical values.

^{1}H-NMR spectrum showed that hexose repeats are from both β-glucan and β-galactan (data not shown). The presence of Glc and Gal were confirmed by the fact that Gal, observed in the monosaccharide analysis, probably originates from β-galactan and β-glucan from snail eggs.

Discussion

The glycans of invertebrates include diverse and often novel structures [13, 17, 18]. Following the change in glycan composition during development and early growth can offer an improved understanding of both invertebrate development and insights into vertebrate biosynthesis and early development. As part of ongoing studies in our

Scheme 1 The simplified *N*-glycan biosynthetic pathway [17, 30]

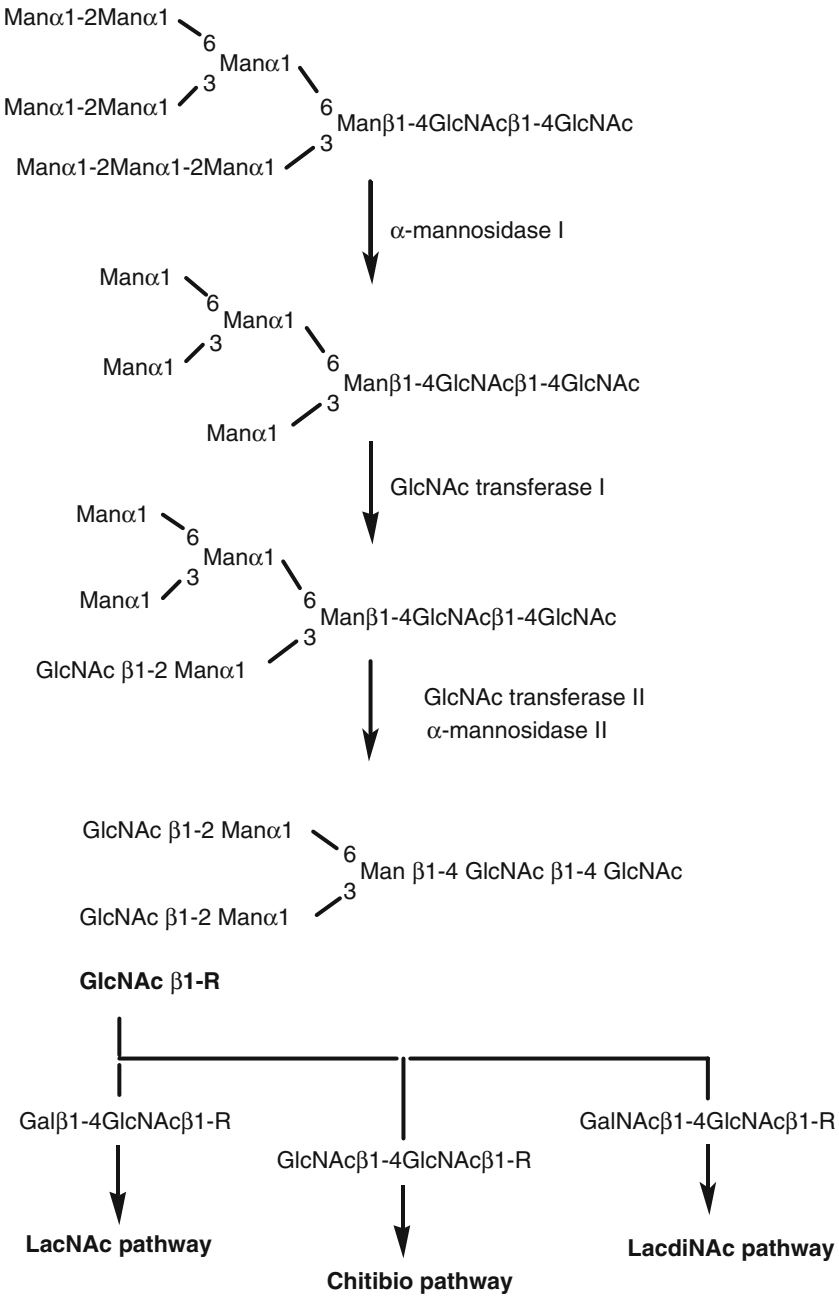

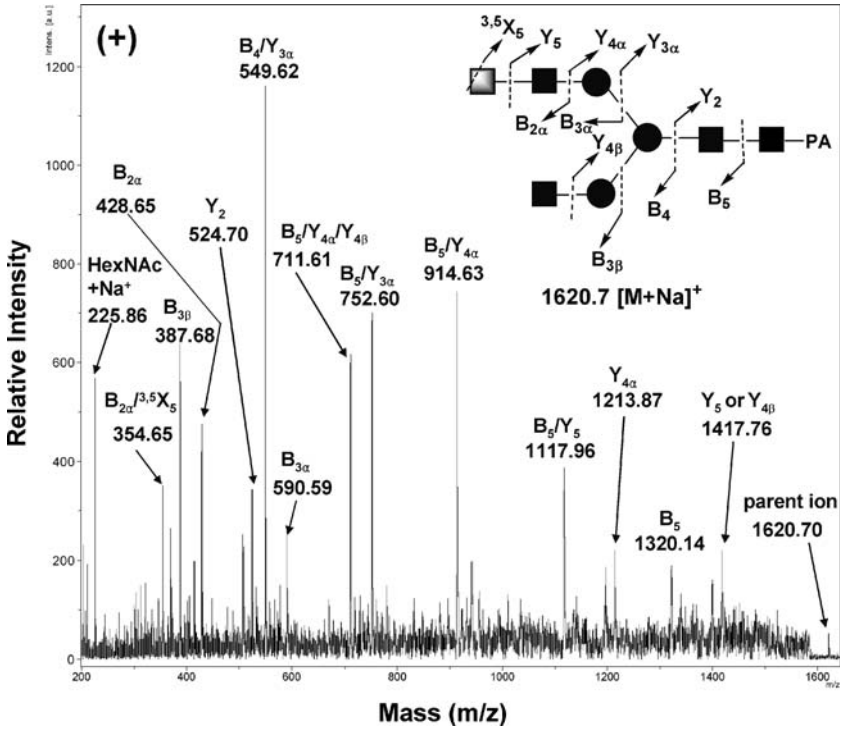

Fig 4 MALDI-MS/MS of complex-type *N*-glycan (Hex_3-$HexNAc_5$-PA) in positive ion mode. One of possible structures was shown for an example. *Filled square* GlcNAc, *circle* Man, *open square* GalNAc

laboratory, we looked at the change in glycan structure in both the eggs and hatchling *Achatina fulica* snails.

Our study surveyed the neutral sugars in the eggs and hatchlings of *Achatina fulica*. Eleven types of monosaccharides (Fuc, Rha, arabinose, GalN, GlcN, Gal, Glc, Man, xylose, ribose, and fructose) had been reported from snail-conditioned water (*Lymnaea truncatula*, and *L. stagnalis* snails) by Kalbe *et al.* [32]. In *Achatina fulica,* seven

Table 4 Assignments of molecular and characteristic fragment ions observed in the MALDI MS/MS of complex type *N*-glycans

Observed signal (*m/z*)	Assignments	Unlabeled	2-PA labeled
225.8	HexNAc + Na^+	0	0
321.3	HexNAc-PA + H_2O + Na^+	–	0
354.7	($HexNAc_2$ + Na^+) minus $^{3,5}X$ cleavage	0	0
387.7	HexHexNAc + Na^+	0	0
428.7	$HexNAc_2$+Na^+	0	0
524.7	$HexNAc_2$-PA + H_2O + Na^+	–	0
549.6	$Hex_2HexNAc$ + Na^+	0	0
590.6	$HexHexNAc_2$ + Na^+	0	0
711.6	$Hex_3HexNAc$ + Na^+	0	0
752.6	$Hex_2HexNAc_2$ + Na^+	0	–
914.6	$Hex_3HexNAc_2$ + Na^+	0	0
932.5	$Hex_3HexNAc_2$ + H_2O + Na^+	0	–
1011.3	$Hex_3HexNAc_2$-PA + H_2O + Na^+	–	0
1117.9	$Hex_3HexNAc_3$ + Na^+	0	0
1135.7	$Hex_3HexNAc_3$ + H_2O + Na^+	0	–
1213.9	$Hex_3HexNAc_3$-PA + H_2O + Na^+	–	0
1320.1	$Hex_3HexNAc_4$ + Na^+	–	0
1338.7	$Hex_3HexNAc_4$ + H_2O + Na^+	0	–
1417.8	$Hex_3HexNAc_4$-PA + H_2O + Na^+	–	0
1541.9	$Hex_3HexNAc_5$ + H_2O + Na^+	0	–
1620.7	$Hex_3HexNAc_5$-PA + H_2O + Na^+	–	0
1745.5	$Hex_3HexNAc_6$ + H_2O + Na^+	0	–
1822.1	$Hex_3HexNAc_6$-PA + H_2O + Na^+	–	0

Table 5 Proposed structures of *N*-glycans and hexose repeats found in *Achatina fulica* eggs. ■, *N*-acetylglucosamine; ●, mannose; □, *N*-acetylgalactosamine; ○, galactose or glucose

(1) Truncated type *N*-glycans

Unlabeled $[M+Na]^+$

theoretical	observed	
771.2	771.3	MALDI-MS
933.3	933.4	
1095.3	1095.4	

2PA-labeled $[M+H]^+$

observed		
827.5	PA	ESI-MS
989.6	PA	ESI-MS/MS
1151.6	PA	

(2) High mannose type *N*-glycans

Unlabeled $[M+Na]^+$

theoretical	observed	
1257.4	1257.5	MALDI-MS
1419.4	1419.5	
1581.5	1581.6	
1743.5	1743.6	
1905.6	1905.6	

0-4

(3) Complex type *N*-glycans (lacdiNAc)[a]

Unlabeled $[M+Na]^+$

theoretical	observed		
1136.6	1136.4	MALDI-MS	
1339.4	1340.5[b]	MALDI-MS/MS	
1542.5	1542.6	MALDI-MS	
1745.6	1745.5	MALDI-MS/MS	

[a]Due to the presence of galactan and glucan contaminants in neutral *N*-glycan preparations, it was not possible to purify one pure compound. Therefore, there are more than one possible structures based on currently accepted *N*-glycan biosynthetic pathway

[b]The observed *m/z* 1340.5 was obtained from Voyage-DE™ STR Biospectrometry Workstation. MALDI-MS/MS was performed on the parent ion at *m/z* 1338.7 with a Bruker Ultraflex III TOF–TOF mass spectrometer

[c]The linear structures were shown. The branched structures may be possible on Hex_4 and Hex_5

monosaccharides were observed in eggs and snails. Moreover, the monosaccharide composition of young snails was more diverse than that in eggs. Gal was present in the highest mole % by day 7–day 10 after hatching. This observation is consistent with the role of galactan in providing nutrition for the growing embryos or the freshly hatched snails. Rha, observed in snails but not in eggs, is also found in surface-layer glycoproteins of prokaryotic

Table 5 (Continued)

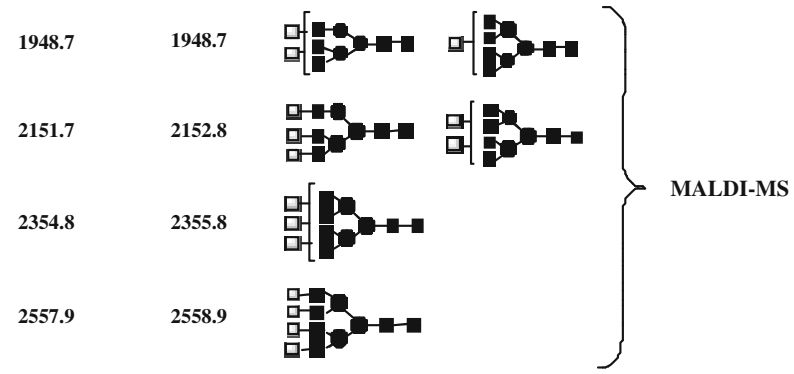

2PA-labeled $[M+Na]^+$

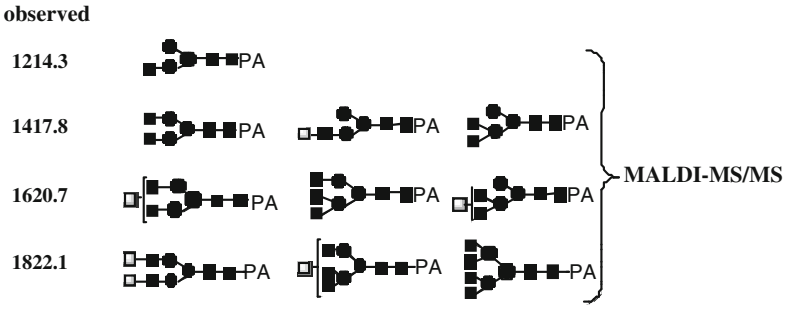

(4) Hexose repeats (copurified with neutral *N*-glycan preparation)[c]

Unlabeled $[M+Na]^+$

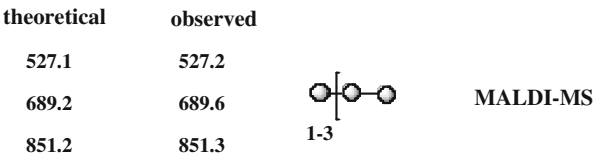

2PA-labeled $[M+H]^+$

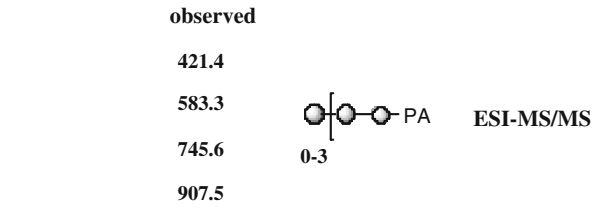

(*Archaea* and bacteria) organisms [33, 34]. Rha might also be derived from *N*- and *O*-linked glycoproteins of snails. Alternatively, Rha might come from the food used for growing the snails, which is composed of rice bran and a commercial product containing the mixture of grains. While natural wheat and rice bran polysaccharides mainly consist of Ara, Xyl, Gal, and Glc, Man and Rha are also present as minor constituents [35]. In mammalian *N*- and *O*-linked oligosaccharides, GlcN (32%), Gal (25%), and Man (19%) are dominant, comprising ~75% of the monosaccharides [36]. *Achatina fulica* snails (~120 days) have GlcN (37%), Gal (19%), and Glc (18%) as major monosaccharides, comprising ~75% of the total monosaccharides.

Our laboratory has been extensively involved in studies [37–43] on a novel GAG that we discovered in 1996 [12].

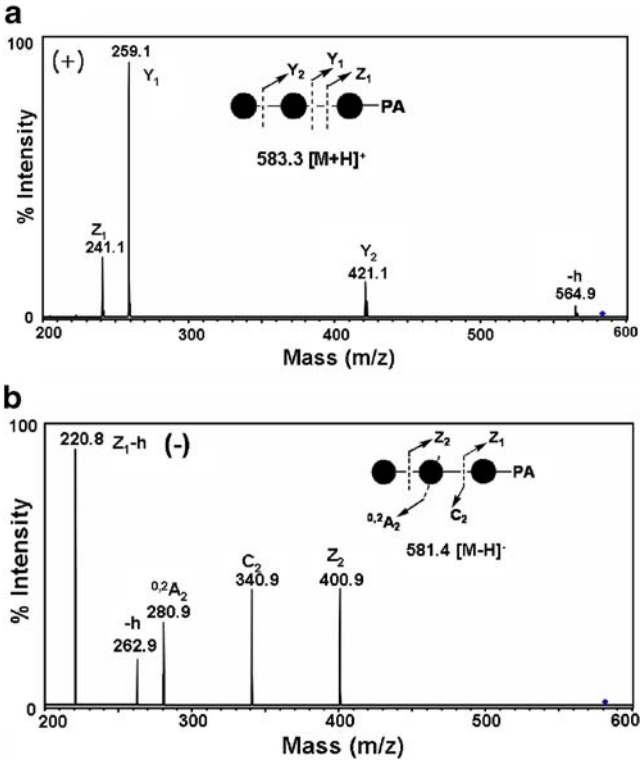

Fig 5 ESI-MS/MS of 2-PA labeled hexose repeats (Hex_3-PA) in **a** positive ion mode, and **b** negative ion mode. *Circle* Gal or Glc

Acharan sulfate has a sequence [→4)-α-D-GlcN*p*Ac (1→4)-α-L-IdoA*p*2S(1→)]$_n$ that is not easily explained based on the currently accepted biosynthetic pathways of GAGs. Acharan sulfate was not observed in eggs suggesting that it was not important in early development. In contrast, the content of acharan sulfate increased continuously after hatching. Acharan sulfate biosynthetic machinery seems to be active immediately following hatching. This suggests that while the GAG acharan sulfate may not be important in snail development, it may play an important role in early snail growth. This is in contrast to GAGs in vertebrates that are essential in early development [1, 44]. The role of acharan sulfate in the early growth of snails may result from its binding, uptake, and transport of divalent cations. Other potential biological roles are as an anti-desiccant, a molecule linked to snail mobility, and an antibiotic molecule [12].

The neutral glycans of *Achatina fulica* were next examined to better understand the source of the monosaccharides that had been identified and to begin to make sense of their role in development and early snail growth. The major neutral *N*-glycans in *Achatina fulica* eggs, released by PNGase F, fell into three types: truncated, high-mannose, and complex (lacdiNAc) types. None of these *N*-glycans carried core fucosylation. The presence of substantial levels of galactans and glucans in eggs made it impossible to purify each *N*-glycan using preparative RP-HPLC. Instead, putative *N*-glycan structures were assigned to each molecular ion on the basis of their composition for a given mass, knowledge of the *N*-glycan biosynthetic pathways, sensitivity towards specific degradative enzymes, monosaccharide compositional analysis, and MS/MS analysis. ESI-MS/MS and MALDI-MS/MS analyses provided detailed structural information on the three types of *N*-glycans as well as their hexose repeats.

A novel UDP-GalNAc:GlcNAc β-R β1–4 *N*-acetylgalactosaminyltransferase had been previously identified from the albumin gland and connective tissue of the snail *Lymnaea stagnalis* [45]. In addition, *Lipidopteran* insect cell lines express a β1→4 *N*-aectylgalactosaminyltransferase, catalyzing the transfer of GalNAc from UDP-GalNAc to oligosaccharides and glycoproteins carrying a non-reducing terminal GlcNAc residue. This suggests that *Lipidopteran* insect cells are capable of synthesizing complex-type lacdiNAc units [46]. Our results suggest that *Achatina fulica* eggs are also synthesizing complex-type lacdiNAc units carrying 1 to 8 HexNAc residues at trimannosyl-chitobiose core. Glycosyltransferase catalyzed addition of α-NeuAc, α-Gal, and β-GlcNAc generally readily occurs at the C-3 of Gal residue in lacNAc. In contrast, these additions appear to proceed at very low rates or not at all to C-3 of the GalNAc residues in lacdiNAc chains [30]. This suggests that polylactosdiaminoglycan [(GalNAcβ1→4GlcNAcβ1→3)$_n$] sequences do not generally occur in nature. Instead, it appears that lacdiNAc type chains are peculiar to the glycoproteins of lower animal species. It has been proposed that lacdiNAc type *N*-glycans at the surface of schistosomes might create a molecular mimicry that contributes to an evasion of the defense system of the snail host resulting in successful infection [47]. Morelle *et al.* [48] reported that *N*-glycans from the nematode *Trichinella spiralis* have phosphorylcholine-containing structures. They also identified multi-antennary lacdiNAc structures with and without core fucosylation.

The monosaccharide composition of snail egg *N*-glycans shows a high mole % of Gal that appears to originate from galactan co-purifying with the *N*-glycans. Galactan is normally found in the albumin gland and in the egg jelly of snails. Nader *et al.* [11] proposed that the acidic galactan may be synthesized from the neutral galactan, already present in the eggs in high amounts, and may replace hyaluronic acid in the mollusc embryogenesis. The substitution of acidic galactans for GAGs in snail egg might explain the absence of the GAG, acharan sulfate, in snail eggs. This further suggests differences in molecules important in the signal transduction and molecular biology of vertebrates and invertebrates. In acidic *N*-glycans, Gal (64.1%) is also highest among the monosaccharides, supporting the presence of

acidic galactan in snail eggs. Glc, observed in the neutral *N*-glycan, is likely derived from glucan oligosaccharides that was co-purified with *N*-glycans (NMR data, not shown). Alternatively, its presence might suggest unprocessed $Man_9GlcNAc_2$, with linked Glc residues, which is not detected in MS analysis. Interestingly, no Fuc was observed in either neutral or acidic *N*-glycans suggesting no (α1–3/ α1–6) fucosylations at chitobiose core, consistent with the neutral *N*-glycan structures confirmed by the MS analysis.

The hexose repeats in neutral *N*-glycan preparation are likely from galactans and are degraded by β-galactanase. It is known that β-galactanase appears on day 7 in development of the invertebrate mollusk *Pomacea* sp. appears to play a role in the degradation of acidic β-galactan to Gal and di- and tri-galactosides [49]. Our MS analysis showed that the neutral *N*-glycans preparation contained 2 to 5 hexose repeats suggesting the degradation of neutral β-galactan with generation of di-, tri-, tetra-, and penta-galactosides. Acidic galactans are at their maximum concentration by day 6 after oviposition in snail hatching, then the concentration slowly decreases and by day 12 they are no longer detectable [11].

In summary, the invertebrate snail displays a complex glycome that differs substantially from the vertebrate one throughout the development and early growth. The regulation of development and energy storage in snail egg appears to be a function of neutral and acidic galactans. Snail GAG acharan sulfate is detected only after hatching and apparently provides other functions such as assembly of the shell from calcium cations, anti-dessication, mobility, and defense. The neutral *N*-glycans include lacdiNAc type structures that carry out other specialized biological functions still to be determined.

Acknowledgements Authors thank Professor Toshihiko Toida of Chiba University for assistance in NMR interpretation. The authors also acknowledge funding from the U.S. National Institutes of Health (grants GM38060 and HL62244) to Robert J. Linhardt, and from the KOSEF grant RO1-1999-2-209-010-5 to YSK. This project was partially supported by the grant from National Institute of Agricultural Biotechnology, Suwon, Republic of Korea.

References

1. Bishop, J.R., Schuksz, M., Esko, J.D.: Heparan sulphate proteoglycans fine-tune mammalian physiology. Nature **446**, 1030–1037 (2007)
2. Cantor, J.O., Nadkarni, P.P.: Hyaluronan: the Jekyll and Hyde molecule. Inflammation and Allergy - Drug Targets **5**, 257–260 (2006)
3. Munoz, E.M., Linhardt, R.J.: Heparin binding domains in vascular biology. Arterioscler. Thromb. Vasc. Biol. **24**, 1549–1557 (2004)
4. Volpi, N.: Chondroitin sulfate structure, role and pharmacological activity. In: Advances in Pharmacology. Elsevier, Amsterdam (2006)
5. Medeiros, G.F., Mendese, A., Castro, R.A.B., Bau, E.C., Nader, H.B., Dietrich, C.P.: Distribution of sulfated glycosaminoglycans in the animal kingdom: widespread occurrence of heparin-like compounds in invertebrates. Biochim. Biophys. Acta **1475**, 287–294 (2000)
6. Nakano, T., Ikawa, N., Ozimek, L.: Extraction of glycosaminoglycans from chicken eggshell. Poult. Sci. **80**, 681–684 (2001)
7. Ha, Y.W., Son, M.J., Yun, K.S., Kim, Y.S.: Relationship between eggshell strength and keratan sulfate of eggshell membranes. Com. Biochem. Physiol. **147A**, 1109–1115 (2007)
8. Toyoda, H., Kinoshita-Toyoda, A., Selleck, S.B.: Structural analysis of glycosaminoglycans in *Drosophila* and *Caenorhabditis elegans* and demonstration that *tout-velu*, a *Drosophila* gene related to EXT tumor suppressors, affects heparan sulfate *in vivo*. J. Biol. Chem. **275**, 2269–2275 (2000)
9. Sinnis, P., Coppi, A., Toida, T., Toyoda, H., Kinoshita-Toyoda, A., Xie, J., Kemp, M.M., Linhardt, R.J.: Mosquito heparan sulfate and its potential role in malaria infection and transmission. J. Biol. Chem. **282**, 25376–25384 (2007)
10. Vilela-Silva, A.-C.E.S., Werneck, C.C., Valente, A.P., Vacquier, V.D., Mourao, P.A.S.: Embryos of the sea urchin *Strongylocentrotus purpuratus* synthesize a dermatan sulfate enriched in 4-*O*- and 6-*O*-disulfated galactosamine units. Glycobiology **11**, 433–440 (2001)
11. Nader, H.B., Jeronimo, S.M.B., Porcionatto, M.A., Dietrich, C.P.: Biosynthesis of an acidic galactan and sulfated glycosaminoglycans during embryonic development of the mollusc *Pomacea* sp. Biochim. Biophys. Acta **840**, 187–192 (1985)
12. Kim, Y.S., Jo, Y.Y., Chang, I.M., Toida, T., Park, Y., Linhardt, R. J.: A new glycosaminoglycan from the giant African snail *Achatina fulica*. J. Biol. Chem. **271**, 11750–11755 (1996)
13. Gutternigg, M., Ahrer, K., Grabher-Meier, H., Burgmayr, S., Staudacher, E.: Neutral *N*-glycans of the gastropode *Arion lusitanicus*. Eur. J. Biochem. **271**, 1348–1356 (2004)
14. Gutternigg, M., Burgmayr, S., Poltl, G., Rudolf, J., Staudacher, E.: Neutral *N*-glycan patterns of the gastropods *Limax maximus*, *Cepaea hortensis*, *Planorbarius corneus*, *Arianta arbustorum* and *Achatina fulica*. Glycoconj. J. **24**, 475–489 (2007)
15. Van Kuik, J.A., Sijbesma, R.P., Kamerling, J.P., Vliegenthart, J.F. G., Wood, E.J.: Primary structure determination of seven novel *N*-linked carbohydrate chains derived from hemocyanin of *Lymnaea stagnalis*. Eur. J. Biochem. **169**, 399–411 (1987)
16. Dreon, M.S., Heras, H., Pollero, R.J.: Characterization of the major egg glycoproteins from the perivitellin fluid of the apple snail *Pomacea canaliculata*. Mol. Reprod. Dev. **68**, 359–364 (2004)
17. Khoo, K.-H., Chatterjee, D., Caulfield, J.P., Morris, H.R., Dell, A.: Structural mapping of the glycans from the egg glycoproteins of *Schistosoma mansoni* and *Schistosoma japonicum*: identification if novel core structures and terminal sequences. Glycobiology **7**, 663–677 (1997)
18. Sandra, K., Dolashka-Angelova, P., Devreese, B., Beeumen, J.V.: New insights *Rapana venosa* hemocyanin *N*-glycosylation resulting from on-line mass spectrometric analyses. Glycobiology **17**, 141–156 (2007)
19. Van Tetering, A., Schiphorst, W.E.C.M., Van den Eijnden, D.H., Van Die, I.: Characterization of a core a1–3 -fucosyltransferase from the snail *Lymnaea stagnails* that is involved in the synthesis of complex-type *N*-glycans. FEBS Lett. **461**, 311–314 (1999)
20. Bretting, H., Whittaker, N.F., Kabat, E.A., Konigsmann-Lange, K., Thiem, H.-J.: Chemical and immunochemical studies on the structure of four snail galactans. Carbohydr. Res. **98**, 213–236 (1981)
21. Uhlenbruck, G., Steinhausen, G., Kareem, H.A.: Different glycosubstances and galactans in the albumin gland and eggs of *Achatina fulica*. Z. Immun.-Forsch. **152**, 220–230 (1976)
22. Lacomini, M., Duarte, G.R., Duarte, E.R., Duarte, H.S., Fontana, J.D., Duarte, J.H.: Structural study on snail galactans from the genus *Biomphalaria*. Agr. Biol. Chem. **45**, 1373–1380 (1981)
23. Hong, S.-W., Shin, H.-Y., Kim, Y.S., Kim, D.-H.: Purification and characterization of novel salt-active acharan sulfate lyase from *Bacteroides stercoris* HJ-15. Eur. J. Biochem. **270**, 3168–3173 (2003)

24. Kim, B.-T., Hong, S.-W., Kim, W.-S., Kim, Y.S., Kim, D.-H.: Purification and characterization of acharan sulfate lyases, two novel heparinases, from *Bacteroides stercoris* HJ-15. Eur. J. Biochem. **268**, 2635–2641 (2001)
25. Lehr, T., Geyer, H., Maab, K., Doenhoff, M.J., Geyer, R.: Structural characterization of *N*-glycans from the fresh water snail *Biomphalaria glabrata* cross-reacting with *Schistosoma mansoni* glycoconjugates. Glycobiology **17**, 82–103 (2006)
26. Packer, N.H., Lawson, M.A., Jardine, D.R., Redmond, J.W.: A general approach to desalting oligosaccharides released from glycoproteins. Glycoconj. J. **15**, 737–747 (1998)
27. Hase, S.: Analysis of sugar chains by phyridylamination. Methods. Mol. Biol.: Glycoprotein analysis in biomedicine **14**, 69–80 (1993)
28. Harvey, D.J.: Collision-induced fragmentation of underivatized *N*-linked carbohydrates ionized by electrospray. J. Mass Spectrom. **35**, 1178–1190 (2000)
29. Domon, B., Costello, C.E.: A systemic nomenclature for carbohydrate fragmentations in FAB-MS/MS spectra of glycoconjugates. Glycoconj. J. **5**, 397–409 (1988)
30. Van den Eijinden, D.H., Neeleman, A.P., Van der Knaap, W.P.W., Bakker, H., Agterberg, M., Van Die, I.: Control and function of complex-type oligosaccharide synthesis: Novel variants of the lacNAc pathway. In: Alavi, A., Axford, J.S. (eds.) Glycoimmunology, pp. 47–52. Plenum, New York (1995)
31. Okamoto, M., Takahashi, K.-I., Doi, T., Takimoto, Y.: High-sensitivity detection and postsource decay of 2-aminopyridine-derivatized oligosaccharides with matrix-assisted laser desorption/ionization mass spectrometry. Anal. Chem. **69**, 2919–2926 (1997)
32. Kalbe, M., Haberl, B., Haas, W.: Snail host finding by *Fasciola hepatica* and *Trichobilharzia ocellata*: compound analysis of "miracidia-attracting glycoproteins". Exp. Parasitol. **96**, 231–242 (2000)
33. Schaffer, C., Graninger, M., Messner, P.: Prokaryotic glycosylation. Proteomics **1**, 248–261 (2001)
34. Christian, R., Schulz, G., Unger, F.M., Messner, P., Kupcu, Z., Sleytr, U.B.: Structure of a rhamnan from the surface -layer glycoprotein of *Bacillus stearothermophilus* strain NRS 2004/3a. Carbohydr. Res. **150**, 265–272 (1986)
35. Hegde, S., Kavitha, S., Varadaraj, M.C., Muralikrishna, G.: Degradation of cereal bran polysaccharide-phenolic acid complexes by *Aspergillus niger* CFR 1105. Food Chem. **96**, 14–19 (2006)
36. Werz, D.B., Ranzinger, R., Herget, S., Adibekian, A., Von der Lieth, C.-W., Seeberger, P.H.: Exploring the structural diversity of mammalian carbohydrates ("glycospace") by statistical databank analysis. ACS Chemical Biol. **2**, 685–691 (2007)
37. Chi, L., Munoz, E.M., Choi, H.S., Ha, Y.W., Kim, Y.S., Toida, T., Linhardt, R.J.: Preparation and structural determination of large oligosaccharides derived from acharan sulfate. Carbohydr. Res. **341**, 864–869 (2006)
38. Jeong, J., Toida, T., Muneta, Y., Kosiishi, I., Immanari, T., Linhardt, R. J., Choi, H.S., Woo, S.J., Kim, Y.S.: Localization and characterization of acharan sulfate in the body of the giant African snail *Achatina fulica*. Comp. Biochem. Physiol. B **130B**, 513–519 (2001)
39. Joo, E.J., Ten Dam, G.B., Van Kuppevelt, T.H., Toida, T., Linhardt, R. J., Kim, Y.S.: Nucleolin: acharan sulfate-binding protein on the surface of cancer cells. Glycobiology **15**, 1–9 (2005)
40. Kim, Y.S., Ahn, M.Y., Wu, S.J., Kim, D.H., Toida, T., Teesch, L. M., Park, Y., Yu, G., Lin, J., Linhardt, R.J.: Determination of the structure of oligosaccharides prepared from acharan sulfate. Glycobiology **8**, 869–877 (1998)
41. Lee, Y.S., Yang, H.O., Shin, K.H., Choi, H.S., Jung, S.H., Kim, Y. M., Oh, D.K., Linhardt, R.J., Kim, Y.S.: Suppression of tumor growth by a new glycosaminoglycan isolated from the African giant snail *Achatina fulica*. Eur. J. Pharmacol. **465**, 191–198 (2003)
42. Li, D.-W., Lee, I.S., Sim, J.-S., Toida, T., Linhardt, R.J., Kim, Y. S.: Long duration of anticoagulant activity and protective effects of acharan sulfate *in vivo*. Thromb. Res. **113**, 67–73 (2004)
43. Wu, S.J., Chun, M.W., Shin, K.H., Toida, T., Park, Y., Linhardt, R.J., Kim, Y.S.: Chemical sulfonation and anticoagulant activity of acharan sulfate. Thromb. Res. **92**, 273–281 (1998)
44. Pallerla, S.R., Pan, Y., Zhang, X., Esko, J.D., Grobe, K.: Heparan sulfate Ndst1 gene function variably regulates multiple signaling pathways during mouse development. Dev. Dyn. **236**, 556–563 (2007)
45. Mulder, H., Spronk, B.A., Schachter, H., Neeleman, A.P., Van den Eijnden, D.H., De Jong-Brink, M., Kamerling, J.P., Vliegenthart, J.F.G.: Identification of a novel UDP-GalNAc:GlcNAcbR b 1–4 *N*-acetylgalactosaminyltransferase from the albumen gland and connective tissue of the snail *Lymnaea stagnalis*. Eur. J. Biochem. **227**, 175–185 (1995)
46. Van Die, I., Van Tetering, A., Bakker, H., Van den Eijnden, D.H., Joziasse, D.H.: Glycosylation in Lepidopteran insect cells: identification of a b1–4 *N*-acetylgalactosaminyltransferase involved in the synthesis of complex-type oligosaccharide chains. Glycobiology **6**, 157–164 (1996)
47. Dissous, C., Grzych, J.M., Capron, A.: *Schistosoma mansoni* shares a protective oligosaccharide epitope with freshwater and marine snails. Nature **323**, 443–445 (1986)
48. Morelle, W., Haslam, S.M., Olivier, V., Appleton, J.A., Morris, H. R., Dell, A.: Phorphorylcholine-containing *N*-glycans of *Trichinella spiralis*: identification of multiantennary lacdiNAc structures. Glycobiology **10**, 941–950 (2000)
49. Oliveira, F.W., Chavante, S.F., Santos, E.A., Dietrich, C.P., Nader, H.B.: Appearance and fate of b-galactanase and a,b-galactosidases, heparan sulfate and chondroitin sulfate degrading enzymes during embryonic development of the Mollusk *Pomacea* sp. Biochim. Biophys. Acta **1200**, 241–248 (1994)